UNSYS digital

The Journal of Instrumentation, Automation and Systems

Flight Characteristics of a Quadrotor Helicopter Using Extra Deflecting Thrusters

Akitaka Imamura[†], Masafumi Miwa[§], and Junichi Hino[§]

[†]Department of Electronics, Information and Communication Engineering Faculty of Engineering, Osaka Sangyo University, Japan

[§]Department of Mechanical Engineering, Faculty of Engineering, University of Tokushima, Japan

Abstract— A quadrotor helicopter (QRH) is a radio control (RC) aircraft that tilts its attitude to generate a horizontal force component to move in a direction. With autonomous control, the attitude control system tilts the airframe against disturbances such as wind. Thus, the attitude of a flying QRH is always slanted. In this study, extra thruster rotors were mounted to maintain the position and horizontal attitude of the QRH. The extra thrusters are tilted to generate a thrust against disturbances without inclination of the airframe. This system is constructed with two ducted fans that can tilt on two axes. It is suitable for precise measurements where the airframe posture needs to stay horizontal.

Keywords—Quadrotor, UAV, ducted fan, extra thruster.

I. Introduction

In recent years, much attention has been given to compact, unmanned aerial vehicles (UAV) of the vertical takeoff and landing (VTOL) type; these radio control (RC) helicopters require no runways and have been used for crop dusting and aerial photography. Such unmanned helicopters can be roughly categorized into single-rotor and multi-rotor types. This study focused on the multi-rotor type, which provides good flight stability and controllability. An aircraft generally tilts its airframe when turning or coping with crosswinds, but tasks such as aerial photography and ground surveys require a horizontal position to be maintained. A common countermeasure is to use a gimbal device to control the angle of the mounted photographic equipment with gyro sensors in order to maintain a constant ground angle even when the attitude of the airframe changes. The objective of this study was to broaden the applicability of the quadrotor helicopter (QRH) through the development of an airframe that enables the aircraft to maintain a horizontal attitude even when moving or being subjected to crosswinds.

As a first step toward achieving this objective, the QRH is proposed to be equipped with extra thrusters (ETs) having a thrust deflection mechanism. An experimental aircraft was prototyped, and its effectiveness was validated through a flight experiment. The fundamental study of the ducted fan (DF) used in this research was previously performed in [3]. A prior study was performed in [5]. Although other researchers have reported on a deflecting-type UAV [2], a UAV using a DF [6], and the relationship between the crosswinds and DF [1], there were no papers available in the literature on a similar study with the same objective.

Corresponding author: A. Imamura (e-mail: imamura@eic.osaka-sandai.ac.jp)
This paper was submitted on September 17, 2014; revised on October 29, 2014; and accepted on November 11, 2014.

II. Moving Attitude of Multirotor

A. Airframe Attitude

Ordinary multirotors have rotors with a fixed pitch. Thus, they require the attack angle of the pitch axis to tilt forward for the vehicle to turn in flight, where the banking angle of the roll axis undergoes the same motion as in a fixed-wing aircraft, as shown in **Figure 1**. The airframe is tilted by the banking angle φ in a circular motion to turn the airframe in order to maintain the centrifugal force F and centripetal force F_o as equal. φ is derived from its relationship with F, as shown in Equations (1) and (2). In order for the aircraft to maintain its altitude while turning, T_R is multiplied n times. n is the load factor, and the additional thrust that becomes necessary is supplemented by increasing the attack angle.

$$F_O = F = T_R \sin\varphi = \frac{W V^2}{g R} \tag{1}$$

$$\varphi = \tan^{-1}\left(\frac{V^2}{g R}\right) \tag{2}$$

$$L = W = T_R \cos\varphi \tag{3}$$

$$n = \frac{T_R}{W} = \frac{1}{\cos\varphi} \tag{4}$$

Because there is no centrifugal force when the aircraft is moving linearly, Equation (1) indicates the force in the horizontal direction. Therefore,

$$F_H = T_R \sin\varphi \tag{5}$$

with the attitude of the aircraft involving the attack angle of the pitch axis leaning forward.

III. Extra Deflecting Thrusters

A. Configuration

Helicopters need to tilt their airframe when moving, turning, or coping with crosswinds. The same is true for a QRH with a simpler mechanism; because the pitch of the rotors is generally fixed, however, stable flight can be achieved by controlling the rotational velocity of the individual rotors.

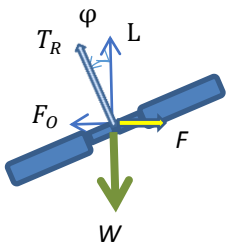

Figure 1 Forces when turning in flight

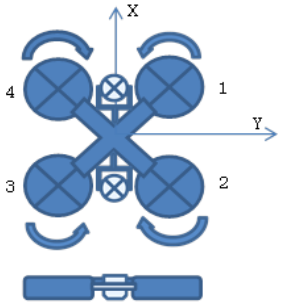

Figure 2 Layout of extra thrusters

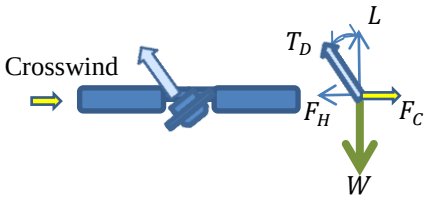

Figure 3 Effect of extra thruster

A gimbal device is usually used to mount equipment such as a camera on a QRH. This device is controlled by a gyro sensor to maintain a horizontal level because the airframe cannot be maintained level at all times. However, this research resolved this problem by fitting ETs that can deflect thrust to make it possible to sustain a level attitude for the airframe. More specifically, two sets of DFs having a gimbal structure are added as ETs on the QRH, as shown in **Figure 2**. **Figure 3** shows how the ET responds to a crosswind.

B. Effects

Mounting ETs has three benefits: a skid effect (horizontal), lift effect (vertical), and stabilization effect.

The skid effect involves coasting the QRH over the surface of a virtual plane with $\varphi = 0$ in order to maintain the attitude of the airframe level at all times. The deflection angle of the ETs θ causes the force while the airframe is in a turning motion to be the same as that given by Equation (1):

$$F_O = F = T_D \sin\theta = \frac{W V^2}{g R} \quad (6)$$

This force becomes a force in the horizontal direction while the airframe is moving linearly or exposed to crosswinds (**Figure 3**). Similar to Equation (5), the following is obtained:

$$F_H = T_D \sin\theta \quad (7)$$

Because the lift is a resultant force of the forces exerted by the rotors and DFs, it becomes

$$L = W = T_R + T_D \cos\theta \quad (8)$$

The stabilizing effect is an effective means of coping with crosswinds caused by turbulence. Deflecting the thrust to face the ETs causes the apparent span to broaden, which increases the robustness against disturbances, as shown in **Figure 4**. Because two sets of ETs are not enough, four sets are needed.

Mounting ETs has the following disadvantages: increased weight, increased electric power consumption, increased complexity of structures and controls, and a high-frequency noise that is characteristic of DFs.

The increased airframe weight is the most significant difficulty. This study considered the skid effect and lift effect, which are relevant to sustaining the horizontal attitude of an airframe.

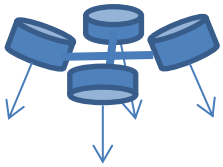

Figure 4 Layout for stabilization effect

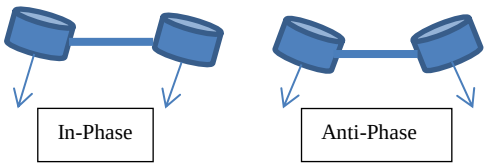

Figure 5 Control methods

IV. CONTROL SYSTEM

A. Deflection Control

As shown in **Figure 5**, there are two methods for controlling the deflection: in the same phase (skid effect) and in opposing phases (stabilization and yaw effects).

Because the prototype experiment was performed using a configuration having a pair of ETs, the scope of this study was limited to in-phase deflection only.

For manual operation of the ETs, automatic control is required to maintain the QRH at a constant altitude while sustaining a horizontal attitude at all times.

B. *Thrust Control*

The thrusts of the DFs are basically kept constant while the deflection angles of the ETs are manipulated, and the force in the horizontal direction is regulated by adjusting the deflection angle of the ETs. Because the lift is affected by the deflection angle, the altitude control of the flight controller is stabilized by using the coefficient

$$n = \frac{1}{\cos\theta} \tag{9}$$

to compensate for T_D. Because the force in the horizontal direction with respect to Equation (7) changes to

$$F_H = \frac{T_D}{\cos\theta}\sin\theta = T_D \tan\theta\ , \tag{10}$$

the operating sensation is different from that for an ordinary QRH.

A. *Control Flow*

The control system can be configured into three flight modes, which are given in **TABLE I**. The manual mode is used for takeoff and landing and for stabilizing the attitude only. The normal mode is used for ordinary flight operation to sustain the altitude and stabilize the attitude.

TABLE I FLIGHT MODE

		Normal Mode	Thruster Mode
QRH	Aileron	Manual Control	Fixation
	Elevator	Manual Control	Fixation
ET	Roll	Automatic Control	Manual Control
	Pitch	Automatic Control	Manual Control

The skid mode is used for operations such as aerial photography, where the flight controller maintains the altitude as in the normal mode. The aileron (roll axis) and elevator (pitch axis) manipulations are disconnected from the remote controller and automatically controlled by the attitude stabilizing feature of the flight controller. The disconnected remote controller is connected to the servo motor, which deflects the roll and pitch angles of the ETs via a transceiver in order to offer a configuration that provides an operating sensation close to that of ordinary controls. **Figures 6** and **7** show the control flows for the normal and skid modes. **Figure 8** shows a block schematic of the altitude sustaining function used in both modes.

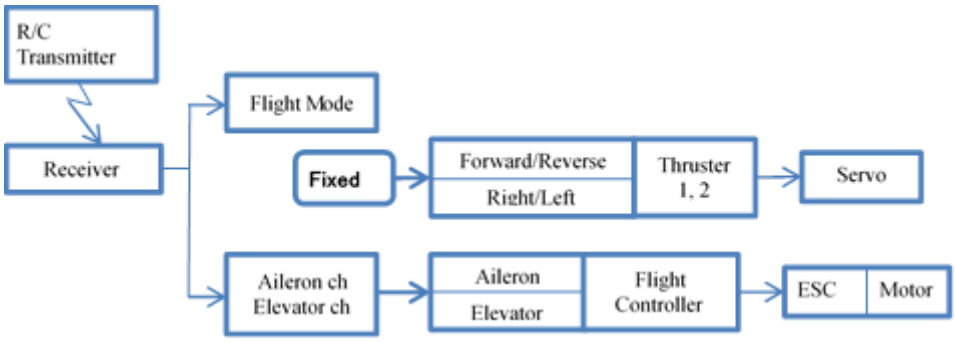

Figure 6 Control flow of normal mode

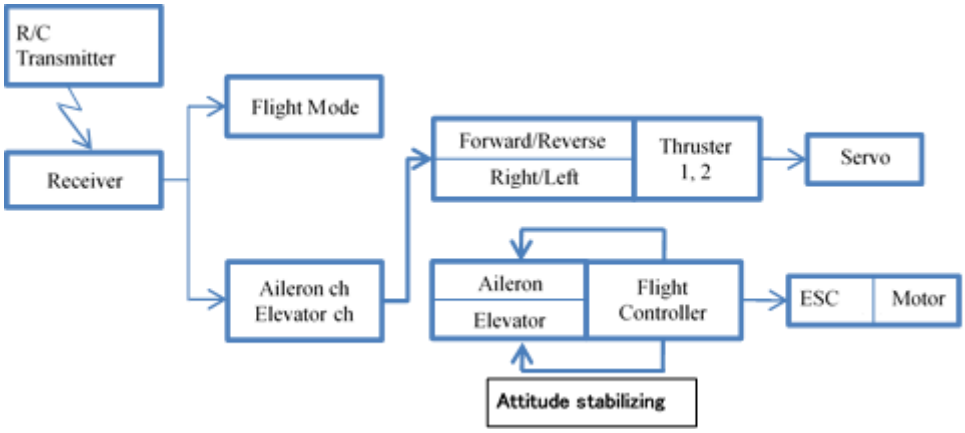

Figure 7 Control flow of skid mode

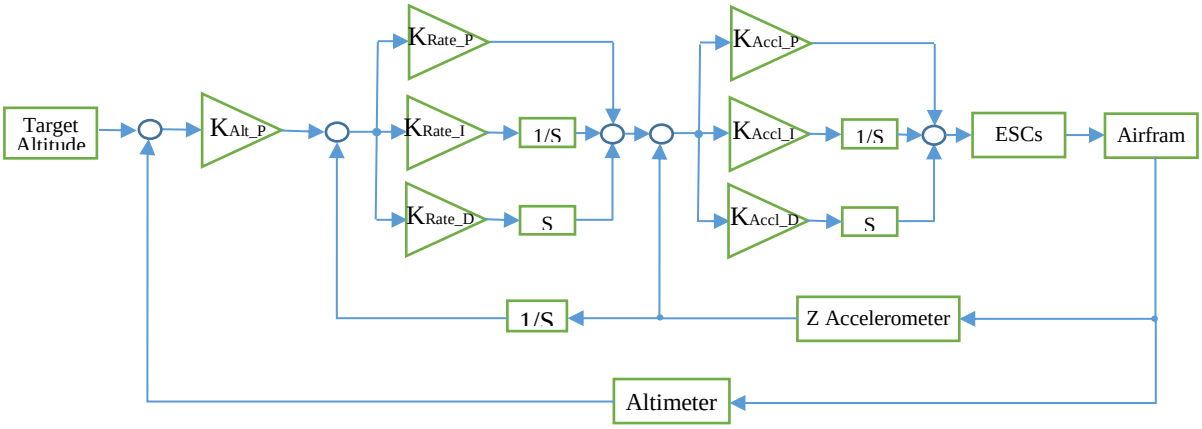

Figure 8 Altitude hold function

Figure 9 Experimental set of QRH

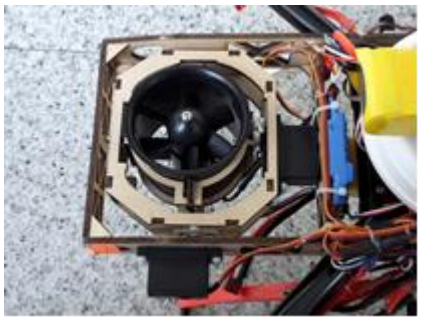

Figure 10 Extra thruster

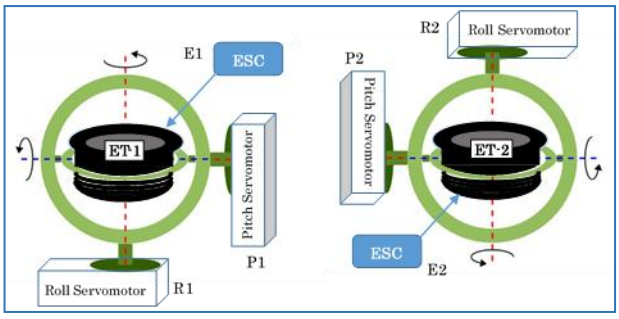

Figure 11 Layout of servo motor for ET

V. EXPERIMENT

A. *Experimental Airframe*

The ETs used in this research were made of a structure that facilitates the deflection of a DF with a gimbal mechanism. One set was installed on each of the left and right sides of the airframe, as shown in **Figures 9** and **10**. A vector nozzle can be considered to be another deflection mechanism; however, because the gimbal mechanism offers a large deflection angle, the airframe can be operated with an angle θ of ±45°. The impellers of the DFs need to be able to move clockwise (CW) and counterclockwise (CCW), just as with rotors. However, because there is little demand for reverse rotation and the selection range is narrow, a DF that was 70 mm in diameter was selected for the experimental aircraft. **TABLE II** presents the specifications of the experimental aircraft, and **TABLE III** presents the specifications of the DF.

Each DF of the ETs comprised a gimbal structure and was driven by two servo motors. **Figure 11** shows the structure of the ETs. The four servo motors and two electric speed controllers (ESC) were controlled by the functions of the RC receiver unit. **TABLE IV** gives the connection, while **TABLE V** presents the program mixing.

Synchronizing the deflection angles of the two sets of ETs is important, and the attitude control of the QRH is affected when this phase coordination is poor. The airframe shifts towards the yaw axis when there is a phase error with the pitch axis of the ETs, while the airframe shifts towards the pitch axis when there is a phase error with the roll axis of the ETs.

B. *Experiment Conditions*

Flight experiments were conducted indoors with the following three conditions to measure the attitude angle of the airframe and the change in angular velocity over time for a statistical evaluation of the attitude stability of the airframe.

TABLE II SPECIFICATIONS OF TEST HELICOPTER

Rotor axis distance	650 [mm]
Rotor diameter	12x3.7 [inch]
Motors	DC Brushless 850 [kV], 656[W]
ESCs	40[A]
Height	250[mm]
Width	500 [mm]
Net weight	2.59 [kg]
LiPo Battery (Weight)	5000mAH-4S-25C x 2 (0.92[kg])

TABLE III SPECIFICATIONS OF DF

Outer diameter (Max.)	83 [mm]
Inside diameter	70 [mm]
Length	58 [mm]
Diameter of impeller	68 [mm]
Number of blades	6
Thrust	1.1 [kgf]
Motors	DC Brushless 3000 [kV]
ESCs	45 [A]

TABLE IV NAME OF SERVO MOTOR AND ESC FOR ET

ET No. (Left / Right)	ET-1 (Left)	ET-2 (Right)
Pitch (RC Ch.)	P1 (Aux2, Reverse)	P2 (Aux3)
Roll (RC Ch.)	R1 (Aux4)	R2 (Aux5, Reverse)
ESC (RC Ch.)	E1 (Aux6)	E2 (Gear)

TABLE V PROGRAM MIXING FOR RC TRANSMITTER

Program No.	Primary > Secondary	Upper Position (%) Lower Position (%)
1	Throttle > E2	High +100 Low +100
2	Throttle > E1	High +100 Low +100
3	Elevator > P1	Down +100 Up +100
4	Elevator > P2	Down +100 Up +100
5	Aileron > R1	Left +100 Right +100
6	Aileron > R2	Left +100 Right +100

1) Experiment 1: Flight experiment involving repeated linear motions back and forth

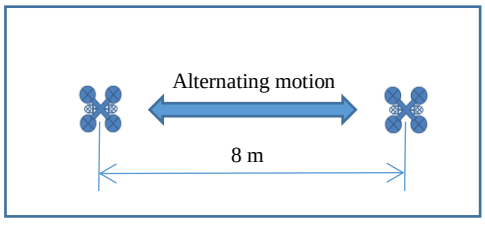

Figure 12 Flight pattern of Experiment 1

Figure 13 Scene from Experiment 1

2) Experiment 2: Flight experiment involving circular motion

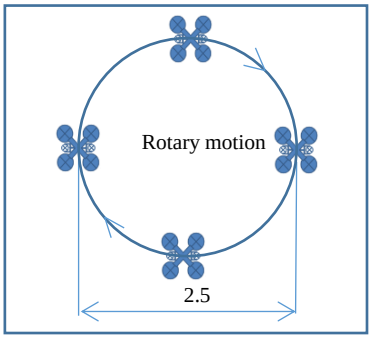

Figure 14 Flight pattern of Experiment 2

3) Experiment 3: Hovering experiment for coping with crosswind

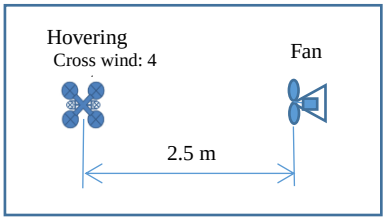

Figure 15 Flight pattern of Experiment 3

Figure 16 Scene from Experiment 3

VI. EXPERIMENT RESULTS

A. Experiment 1

Experiment 1 was conducted by flying the experimental aircraft between two points indoors while measuring the attitude angle of the airframe and change in angular velocity. **Figure 17** shows the attitude angle, and **Figure 18** shows the

angular velocity. **TABLES VI** and **VII** present their statistical evaluations. The measurement data were sampled at 10 Hz.

The flight involved takeoff in manual mode at t = 60 s, a transition to normal mode at t = 112 s, and a shift to skid mode at t = 170 s. Large peak values were generated with the pitch angle when the aircraft turned around in normal mode, as shown in **Figure 15**. The variation range was quite broad. In contrast, the peak values were small when the aircraft turned around in skid mode, and the range was narrow. A comparison of these two flight modes showed that the skid mode reduced the standard deviations in the attitude angle and angular velocity by 22.5%–30.3% and 24.8%–51.1%, respectively. The average value was not in the proximity of zero because of the phase error of the ETs, as described above.

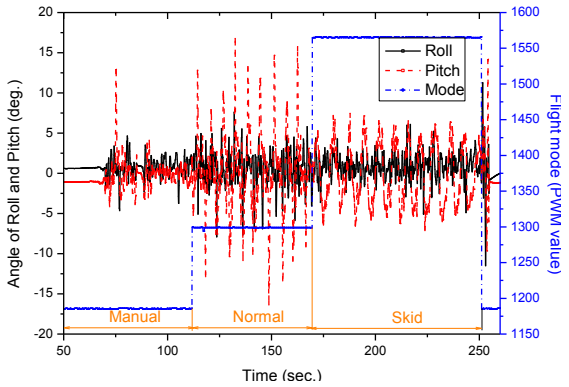

Figure 17 Attitude angle of airframe in Experiment 1

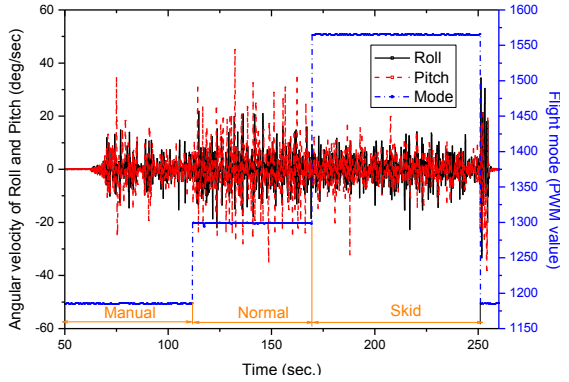

Figure 18 Angular velocity of airframe in Experiment 1

B. *Experiment 2*

Experiment 2 was conducted by flying the experimental aircraft in a circular motion indoors to evaluate the stability when the nose of the aircraft was kept facing the front of the operator instead of turning to generate a certain level of steering at all times. The measurement conditions were the same as those for Experiment 1. **Figure 19** shows the attitude angle, and **Figure 20** shows the angular velocity. Their statistical evaluations are given in **TABLES VIII** and **IX**.

TABLE VI STATISTICAL COMPARISON OF ANGLES IN EXPERIMENT 1

	Normal Mode		Skid Mode	
	Roll	Pitch	Roll	Pitch
Mean	0.52198	0.07548	0.83058	-0.0269
Std. Dev. (Skid/Norm)	2.0903	4.70375	1.45709 (0.697)	3.65987 (0.778)
Min.	-7.92283	-16.37003	-5.10507	-7.12958
Max.	7.64355	16.79715	6.11874	7.48434
Range (Skid/Norm)	15.56638	33.16717	11.22382 (0.721)	14.61392 (0.441)

Range = Max–Min [Unit: deg]

TABLE VII STATISTICAL COMPARISON OF ANGULAR VELOCITIES IN EXPERIMENT 1

	Normal Mode		Skid Mode	
	Roll	Pitch	Roll	Pitch
Mean	-0.24031	-0.11221	0.16329	-0.08135
Std. Dev. (Skid/Norm)	6.41032	9.89405	4.81893 (0.752)	4.83518 (0.489)
Min.	-22.00564	-34.86712	-22.73734	-32.18421
Max.	21.92705	45.10197	14.06124	19.88869
Range (Skid/Norm)	43.93269	79.96908	36.79858 (0.838)	52.0729 (0.651)

Range = Max–Min [Unit: deg/s]

The flight involved takeoff in manual mode at t = 8 s, a transition to normal mode at t = 23 s, and a shift to skid mode at t = 42 s. Because a certain level of steering was present at all times, no peaks were seen for both modes. The skid mode reduced the standard deviations of the attitude angle and angular velocity by 38.7%–60.9% and 45.1%–50.1%, respectively.

It was difficult to maintain a circular motion like the one depicted in **Figure 13** during actual flight. This was partly due to the limited width of the experiment station (4.2 m), so the amount of movement in the left and right directions tended to remain small.

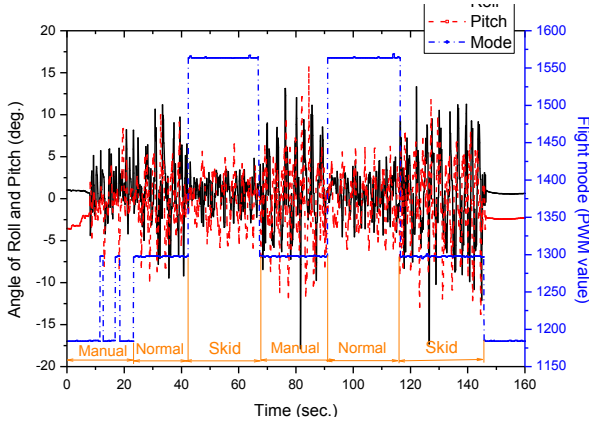

Figure 19 Attitude angle of airframe in Experiment 2

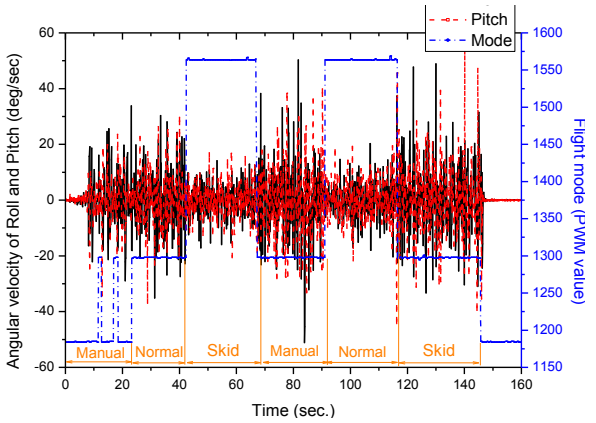

Figure 20 Angular velocity of airframe in Experiment 2

TABLE VIII STATISTICAL COMPARISON OF ANGLES IN EXPERIMENT 2

	Normal Mode		Skid Mode	
	Roll	Pitch	Roll	Pitch
Mean	0.71229	-0.24224	0.6277	-0.14772
Std. Dev. (Skid/Norm)	4.67143	4.46146	1.82593 (0.391)	2.75163 (0.617)
Min.	-17.87238	-13.77044	-4.56198	-6.15831
Max.	13.34099	15.70786	4.98311	6.54467
Range (Skid/Norm)	31.21337	29.4783	9.5451 (0.306)	12.70298 (0.431)

Range = Max–Min [Unit: deg]

TABLE IX STATISTICAL COMPARISON OF ANGULAR VELOCITIES IN EXPERIMENT 2

	Normal Mode		Skid Mode	
	Roll	Pitch	Roll	Pitch
Mean	0.04042	0.19548	-0.13931	0.16166
Std. Dev. (Skid/Norm)	12.21111	11.66438	6.09541 (0.499)	6.4026 (0.549)
Min.	-35.16201	-39.5425	-20.28404	-21.79874
Max.	50.38632	56.18865	20.3255	19.60348
Range (Skid/Norm)	85.54833	95.7312	40.60954 (0.475)	41.40222 (0.432)

Range = Max–Min [Unit: deg/s]

C. Experiment 3

Experiment 3 involved the installation of an industrial fan to evaluate the stability of a hovering flight at a position 2.5 m away from the fan. The measurement conditions were the same as those for Experiment 1. **Figure 21** shows the attitude angle, and **Figure 22** shows the angular velocity. Their statistical evaluations are given in **TABLES X** and **XI**.

The flight involved takeoff in manual mode at t = 54 s, a transition to normal mode at t = 60 s, and a shift to skid mode at t = 79 s. The variation in the pitch axis was large because the front of the airframe was upstream of the wind, but a small amount of variation was also confirmed for the roll axis. The skid mode reduced the standard deviations of the attitude angle and angular velocity by 36.7%–48.6% and 43.8%–52.0%, respectively.

The variation was expected to be small with the roll axis as it was orthogonal to the direction of the wind generated by the fan; however, it was unexpectedly large. This may have been because of turbulence created by the wind bouncing off walls.

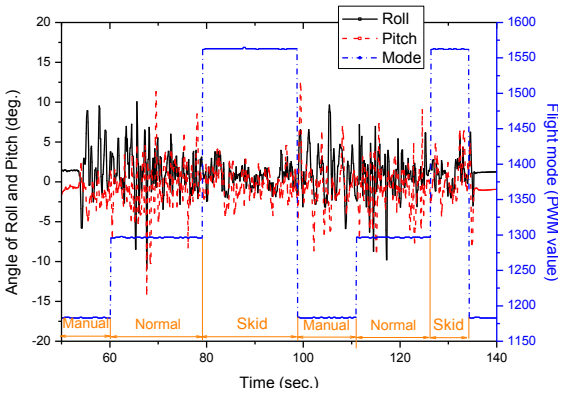

Figure 21 Attitude angle of airframe in Experiment 3

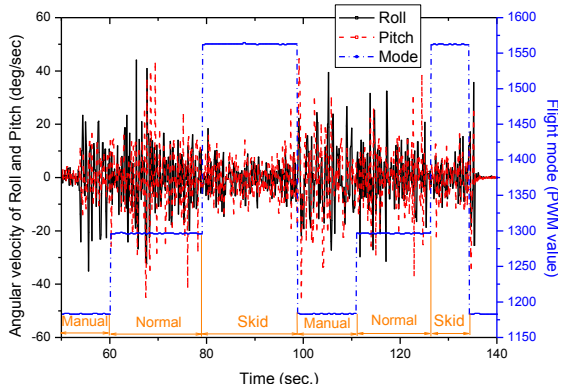

Figure 22 Angular velocity of airframe in Experiment 3

D. Operating Sensations

Because the ETs are only functioned as auxiliary thrusts when the flight mode was in normal mode, their operation made the airframe feel like it became lighter. During skid mode, the control of the QRH relied on the flight controller. The airframe performed horizontal movements as planned when the ETs were manually manipulated, but the operating sensations were peculiar, with the aircraft feeling as if it was sliding on a sheet of ice.

When the use of the ETs was forcibly combined with normal mode, the airframe assumed an angle that reached equilibrium between the deflection angle of the DFs and attitude angle of the controls. This resulted in stabilized hovering with the airframe tilted. When attempts were made with the controls to forcibly roll or pitch the airframe to level it, the airframe moved horizontally to the scheduled direction.

There was an accident involving the airframe tumbling during the experimental flight. This may have been caused by the control failing as some calculations diverged because of the attitude stabilization function of the flight controller remaining

active while the skid mode was used when the aircraft was subjected to strong winds.

TABLE X STATISTICAL COMPARISON OF ANGLES IN EXPERIMENT 3

	Normal Mode		Skid Mode	
	Roll	Pitch	Roll	Pitch
Mean	1.04255	-0.62832	0.69444	-0.01303
Std. Dev. (Skid/Norm)	2.75305	3.15114	1.4138 (0.514)	1.99458 (0.633)
Min.	-10.97661	-14.0856	-2.44423	-4.27597
Max.	10.06559	11.31755	5.77862	6.38602
Range (Skid/Norm)	21.04219	25.40315	8.22285 (0.391)	10.66199 (0.420)

Range = Max–Min [Unit: deg]

TABLE XI STATISTICAL COMPARISON OF ANGULAR VELOCITIES IN EXPERIMENT 3

	Normal Mode		Skid Mode	
	Roll	Pitch	Roll	Pitch
Mean	0.13963	-0.35004	-0.36383	-0.40858
Std. Dev. (Skid/Norm)	11.06123	11.99683	5.31219 (0.480)	6.73642 (0.562)
Min.	-32.37597	-44.84267	-14.57119	-22.22084
Max.	44.11753	42.96174	18.41644	25.67525
Range (Skid/Norm)	76.4935	87.80441	32.98763 (0.431)	47.89609 (0.545)

Range = Max–Min [Unit: deg/s]

VII. Conclusion

The airframe was experimentally confirmed to move horizontally when the ETs mounted on the QRH were operated. While skid mode produced a small difference compared to normal mode statistically, the effects were clearly observed visually. The operating sensations in skid mode were clearly different, but mastering the operation did not take much time.

The horizontal movements and compensation for crosswinds in skid mode as presented in this paper can be implemented to providing new modes for application to aerial photography or ground surveys. However, this will involve complex mechanisms and additional weight. With camera gimbals being equipped with higher levels of functionality these days, a large number of improvements are needed to make this method ready for practical application.

The issues presented in this paper can potentially be resolved through various approaches: changing the thrust mechanism to ducted fans (DF) to create a quad ducted fan helicopter (QDH) [8], where the thrust of the DF is deflected with a vector nozzle; and adding a tilt mechanism to each rotor of the QRH to create a quad tilt rotor helicopter (QTRH) [4, 7] with only one axis used for deflection.

Because all methods have their own advantages and disadvantages, methods that are suitable for a specific purpose need to be considered. In future work, QDH and QTRH prototypes will be developed, and their effectiveness will be examined in experimental flights. The results of the three methods, including the extra thrust method introduced in this paper, will be compared.

References

[1] J. Fleming and T. Jones, "Improving control system effectiveness for ducted fan VTOL UAVs operating in crosswinds," in *2nd AIAA "Unmanned Unlimited" Conf. and Workshop & Exhibit*, 2003-6514, 2003.

[2] M. Kumon, H. Cover, and J. Katupitiya, "Hovering control of vectored thrust aerial vehicles," in *IEEE Int. Conf. on Robotics and Automation*, 2010, pp. 1149–1154.

[3] M. Miwa, Y. Shigematsu, and T. Yamashita, "Control of ducted fan flying object using thrust vectoring," *J. Syst. Des. Dyn.*, vol. 6, no. 3, pp. 322–334, Jun. 2012.

[4] M. Ryll, H. H. Bülthoff, and P. R. Giordano, "Modeling and control of a quad rotor UAV with tilting propellers," in *IEEE Int. Conf. on Robotics and Automation*, 2012, pp. 4606–4613.

[5] A. Imamura, M. Miwa, J. Hino, and J-H. Shim, "Extra thruster for quad rotor helicopter," in *Proc. of the 8th Int. Soc. of Intelligent Unmanned Systems (ISIUS)*, 2012, pp. 587–591.

[6] M. Miwa, S. Uemura, Y. Ishihara, J.-H. Shim, A. Imamura, and K. Ioi, "Attitude control of quad ducted-fan helicopter," in *Proc. of the 8th Int. Soc. of Intelligent Unmanned Systems (ISIUS)*, 2012, pp. 280–284.

[7] M. Ryll, H. H. Bülthoff, and P.R. Giordano, "First flight tests for a quad rotor UAV with tilting propellers," in *IEEE Int. Conf. on Robotics and Automation (ICRA)*, 2013, pp. 295-302.

[8] A. Imamura, S. Uemura, M. Miwa, and J. Hino, "Flight characteristics of quad ducted fan helicopter with thrust vectoring nozzles," in *Proc. of the 9th Int. Conf. of Intelligent Unmanned Systems*, ICIUS-2013-034, 2013.